

$(\mu_2\text{-Adipato-}\kappa^4\text{O},\text{O}':\text{O}'',\text{O}''')$ bis[aqua(benzene-1,2-diamine- $\kappa^2\text{N},\text{N}'$)chloridocadmium]: crystal structure and Hirshfeld surface analysis

Wannur Sofiasalamah Khairiah A. Rahman,^a J. Ahmad,^{a,b} Siti Nadiah Abdul Halim,^{a,†} Mukesh M. Jotani^c and Edward R. T. Tiekink^{d,*}

Received 6 August 2017

Accepted 8 August 2017

Edited by W. T. A. Harrison, University of Aberdeen, Scotland

† Additional correspondence author, e-mail: nadiahhalim@um.edu.my

Keywords: crystal structure; cadmium; adipic acid; benzene-1,2-diamine; hydrogen bonding.

CCDC reference: 1446968

Supporting information: this article has supporting information at journals.iucr.org/e

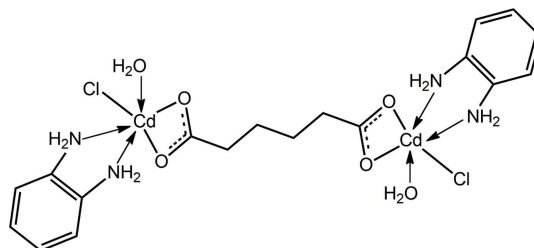
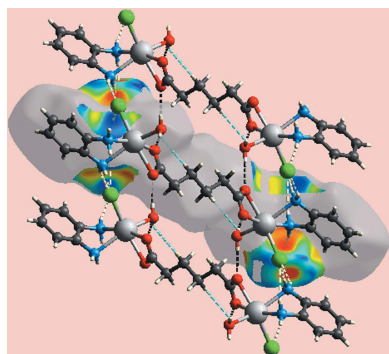
^aDepartment of Chemistry, University of Malaya, 50603 Kuala Lumpur, Malaysia, ^bDepartment of Chemistry, Kulliyah of Science, International Islamic University Malaysia, 25200 Kuantan, Pahang, Malaysia, ^cDepartment of Physics, Bhavan's Sheth R. A. College of Science, Ahmedabad, Gujarat 380 001, India, and ^dResearch Centre for Crystalline Materials, School of Science and Technology, Sunway University, 47500 Bandar Sunway, Selangor Darul Ehsan, Malaysia.

*Correspondence e-mail: edwardt@sunway.edu.my

The full molecule of the binuclear title compound, $[\text{Cd}_2\text{Cl}_2(\text{C}_6\text{H}_8\text{O}_4)(\text{C}_6\text{H}_8\text{N}_2)_2(\text{H}_2\text{O})_2]$, is generated by the application of a centre of inversion located at the middle of the central $\text{CH}_2\text{—CH}_2$ bond of the adipate dianion; the latter chelates a Cd^{II} atom at each end. Along with two carboxylate-O atoms, the Cd^{II} ion is coordinated by the two N atoms of the chelating benzene-1,2-diamine ligand, a Cl^- anion and an aqua ligand to define a distorted octahedral CdClN_2O_3 coordination geometry with the monodentate ligands being mutually *cis*. The disparity in the Cd—N bond lengths is related to the relative *trans* effect exerted by the Cd—O bonds formed by the carboxylate-O and aqua-O atoms. The packing features water-O—H \cdots O(carboxylate) and benzene-1,2-diamine-N—H \cdots Cl hydrogen bonds, leading to layers that stack along the *a*-axis direction. The lack of directional interactions between the layers is confirmed by a Hirshfeld surface analysis.

1. Chemical context

In the +II oxidation state, the $4d^{10}$ cadmium(II) cation is a favourite of researchers studying coordination polymers/metal–organic frameworks. With the ability to readily coordinate a variety of different donor atoms, *i.e.* both hard and soft donors, and to adopt a range of coordination geometries, a diverse array of structures can be generated. The motivation for studying cadmium(II) compounds in this context, over and above intellectual curiosity, rests primarily with evaluating their photoluminescence properties (Lestari *et al.*, 2014; Xue *et al.*, 2015; Seco *et al.*, 2017).



Our interest in cadmium(II) structural chemistry is in the controlled formation (dimensionality and topology) of coordination polymers of dithiophosphates ($\text{S}_2\text{P}(\text{OR})_2$; Lai & Tiekink, 2004, 2006), xanthates (S_2COR ; Tan, Azizuddin *et al.*, 2016) and dithiocarbamates (S_2CNR_2 ; Chai *et al.*, 2003), in particular those substituted with hydroxyethyl groups, capable of forming hydrogen-bonding interactions (Tan *et al.*,

Table 1
Selected bond lengths (Å).

Cd—O1	2.3448 (17)	Cd—N2	2.398 (2)
Cd—O2	2.3560 (16)	Cd—Cl1	2.5283 (6)
Cd—N1	2.448 (2)	Cd—O1W	2.2265 (18)

2013; Tan, Halim & Tiekink, 2016). In this connection, we now describe the crystal structure determination and Hirshfeld surface analysis of a cadmium(II) species, (I), with a potentially bridging adipato dianion and an ancillary ligand, benzene-1,2-diamine, capable of forming hydrogen-bonding interactions.

2. Structural commentary

The asymmetric unit of (I) comprises half a molecule of (I), Fig. 1, with the full molecule generated about a centre of inversion. The key feature of the structure is the tetra-coordinate mode of coordination of the adipato dianion, linking the two Cd^{II} cations. Each carboxylate group forms equivalent Cd—O bonds, the difference in the two bonds being only 0.01 Å, Table 1. More asymmetry is found in the coordination of the benzene-1,2-diamine ligand with the Cd—N1 bond length being 0.05 Å longer than Cd—N2. This may be traced to the different *trans* effects exerted by the oxygen atoms in that the N1 atom is *trans* to the carboxylate-O1 atom [N1—Cd—O1 = 166.89 (6)°] whereas N2 is opposite to the coordinating water molecule [N2—Cd—O1W = 149.12 (7)°]. The coordination geometry is completed by the chloride anion which, owing to the presence of two chelating ligands, occupies a position *cis* to the aqua group. The donor set is ClN₂O₃ and defines a distorted octahedral geometry.

As might be expected, the four-membered chelate ring formed by the carboxylate group is strictly planar (r.m.s. deviation = 0.0009 Å). There is a twist in the chain of the dicarboxylate ligand with the bond linking the quaternary atom to the aliphatic group being + *anti-clinal*, *i.e.* the O2—C1—C2—C3 torsion angle is 145.7 (3)° but, - *anti-periplanar* about the central bond, *i.e.* C1—C2—C3—C3ⁱ is -177.6 (3)°; symmetry code: (i) $-x, 2 - y, -z$. There is a distinct kink in the five-membered ring formed by the benzene-1,2-diamine ligand. This is readily seen in the dihedral angle of 58.57 (7)° formed between the plane through the CdN₂ atoms and the benzene ring.

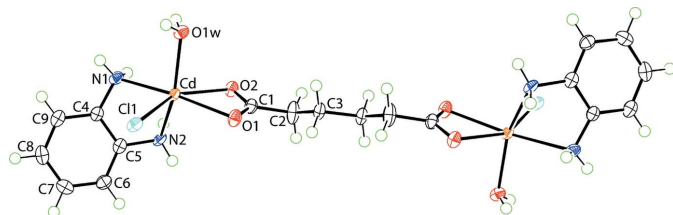


Figure 1
The molecular structure of (I), showing the atom-labelling scheme and displacement ellipsoids at the 70% probability level. The molecule is disposed about a centre of inversion and unlabelled atoms are related by the symmetry operation $(-x, 2 - y, -z)$.

Table 2
Hydrogen-bond geometry (Å, °).

<i>D</i> —H··· <i>A</i>	<i>D</i> —H	H··· <i>A</i>	<i>D</i> ··· <i>A</i>	<i>D</i> —H··· <i>A</i>
O1W—H1W···O1 ⁱ	0.83 (2)	1.90 (2)	2.728 (2)	176 (3)
O1W—H2W···O2 ⁱⁱ	0.83 (1)	1.84 (1)	2.670 (2)	177 (3)
N1—H1N···Cl1 ⁱ	0.88 (2)	2.57 (2)	3.428 (2)	166 (2)
N1—H2N···Cl1 ⁱⁱⁱ	0.88 (2)	2.52 (2)	3.374 (2)	165 (2)
N2—H3N···Cl1 ⁱⁱⁱ	0.87 (2)	2.53 (2)	3.385 (2)	168 (2)
N2—H4N···Cl1 ^{iv}	0.88 (2)	2.52 (2)	3.322 (2)	153 (3)

Symmetry codes: (i) $x, y - 1, z$; (ii) $x, -y - \frac{1}{2}, z - \frac{1}{2}$; (iii) $x, -y - \frac{1}{2}, z - \frac{3}{2}$; (iv) $x, -y + \frac{1}{2}, z - \frac{3}{2}$.

3. Supramolecular features

As summarized in Table 2, all acidic hydrogen atoms in the molecule of (I) are involved in conventional hydrogen-bonding interactions. The water-H atoms each form an hydrogen bond with a carboxylate-O atom to form strands

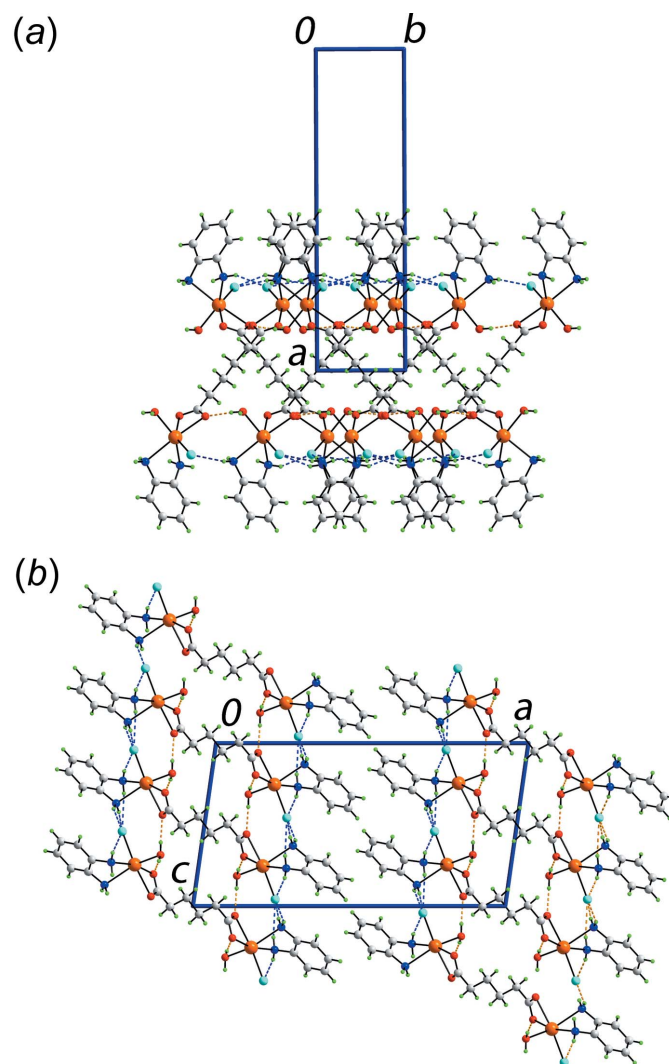


Figure 2
Molecular packing in (I): (a) a view of the supramolecular layer parallel to (100) sustained by water-O—H···O(carboxylate) and benzene-1,2-diamine-N—H···Cl hydrogen bonds and (b) a view of the unit-cell contents in projection down the *b* axis. The O—H···O and N—H···Cl hydrogen bonds are shown as orange and blue dashed lines, respectively.

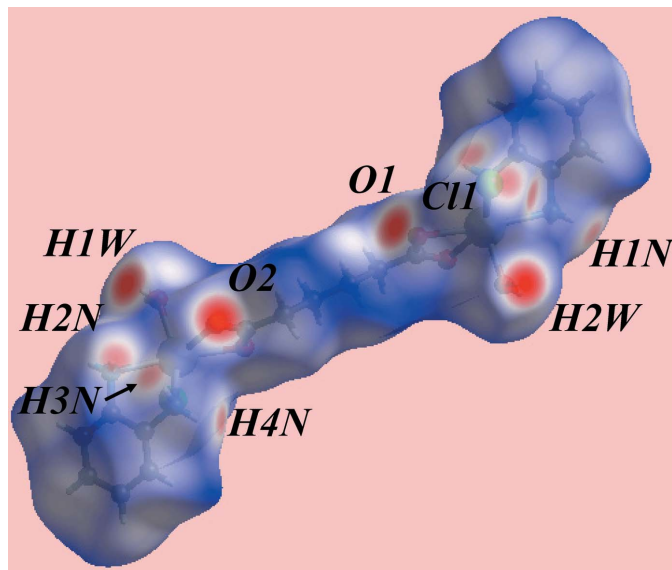


Figure 3
A view of the Hirshfeld surface for (I) mapped over d_{norm} in the range -0.597 to $+1.425$ au.

propagating along the b -axis direction, involving the carboxylate-O1 atoms, and along the c -axis direction, involving the carboxylate-O2 atoms. Thereby, a supramolecular layer is formed parallel to (100), Fig. 2*a*. Within this framework are benzene-1,2-diamine-N—H \cdots Cl hydrogen bonds involving all the amine-H atoms. This has the result that each chloride anion accepts four N—H \cdots Cl hydrogen bonds and, to a first approximation exists in a flat, bowl-shaped environment defined by a CdH₄ ‘donor set’. Layers stack along the a axis with no directional interactions between them, Fig. 2*b*.

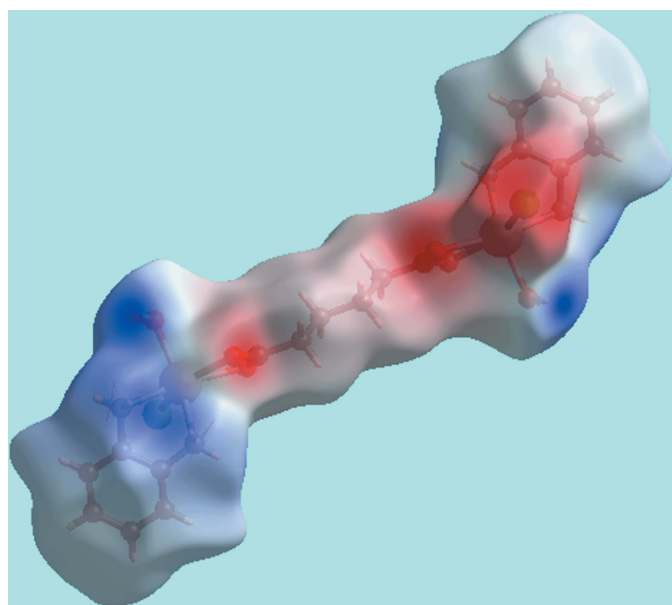


Figure 4
A view of the Hirshfeld surface for (I) mapped over the electrostatic potential in the range -0.164 to $+0.204$ a.u. The red and blue regions represent negative and positive electrostatic potentials, respectively.

Table 3
Percentage contributions of inter-atomic contacts to the Hirshfeld surfaces for (I).

Contact	Percentage contribution
H \cdots H	45.4
O \cdots H/H \cdots O	22.9
Cl \cdots H/H \cdots Cl	19.0
C \cdots H/H \cdots C	11.2
C \cdots Cl/Cl \cdots C	0.7
C \cdots C	0.4
Cl \cdots O/O \cdots Cl	0.3
Cd \cdots H/H \cdots Cd	0.1

Given this observation, it was thought worthwhile to perform a Hirshfeld surface analysis to probe the molecular packing in more detail. The results of this analysis are discussed in the next section.

4. Hirshfeld surface analysis

The Hirshfeld surfaces calculated for (I) provide further insight into the supramolecular associations in the crystal; the calculations were performed according to a recent publication (Jotani *et al.*, 2017). The presence of bright-red spots appearing near water-H atoms, H1W and H2W, and carboxylate oxygen atoms, O1 and O2, on the Hirshfeld surface mapped over d_{norm} in Fig. 3, result from the O—H \cdots O hydrogen bonds between these atoms, Table 2. The faint-red spots appearing near each of diamine-hydrogen atoms, H1N—H4N, and those near the Cl1 atom represent the formation of the four comparatively weak N—H \cdots Cl interactions. The donors and acceptors of above intermolecular interactions can also be viewed as blue and red regions around the respective

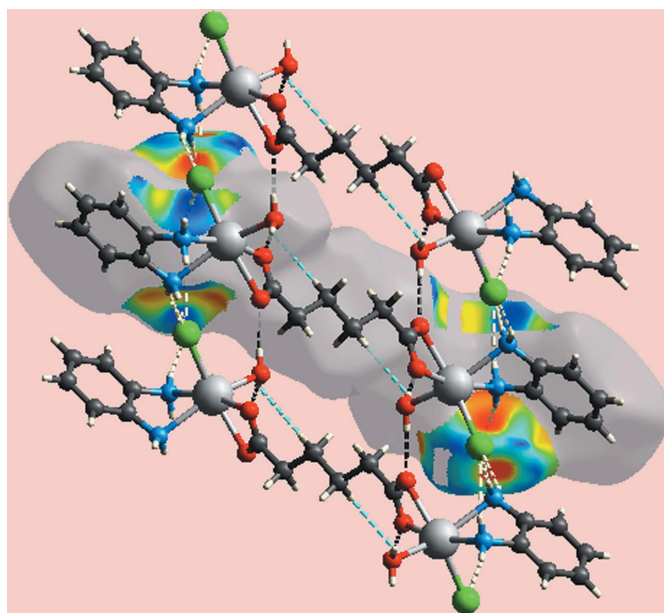


Figure 5
A view of the Hirshfeld surface for (I) mapped with the shape-index property about a reference molecule showing intermolecular O—H \cdots O and N—H \cdots Cl contacts as well as short interatomic H \cdots H contacts as black, white and sky-blue dashed lines, respectively.

Table 4
 Summary of short inter-atomic contacts (Å) in (I).

Contact	Distance	Symmetry operation
H1W...H3A	2.32	$x, -1 + y, z$
H8...H8	2.38	$1 - x, -y, 1 - z$
O1W...H3A	2.64	$x, -1 + y, z$

atoms on the Hirshfeld surface mapped over the calculated electrostatic potential in Fig. 4. The immediate environment about a reference molecule within the shape-index mapped Hirshfeld surface highlighting intermolecular O—H...O, N—H...Cl interactions and short interatomic H...H contacts is illustrated in Fig. 5.

The overall two-dimensional fingerprint plot, Fig. 6a, and those delineated into H...H, O...H/H...O, Cl...H/H...Cl and C...H/H...C contacts (McKinnon *et al.*, 2007) are illustrated in Fig. 6b–e, respectively. The significant contributions from interatomic O...H/H...O and Cl...H/H...Cl contacts to the Hirshfeld surfaces, see data in Table 3, result from the

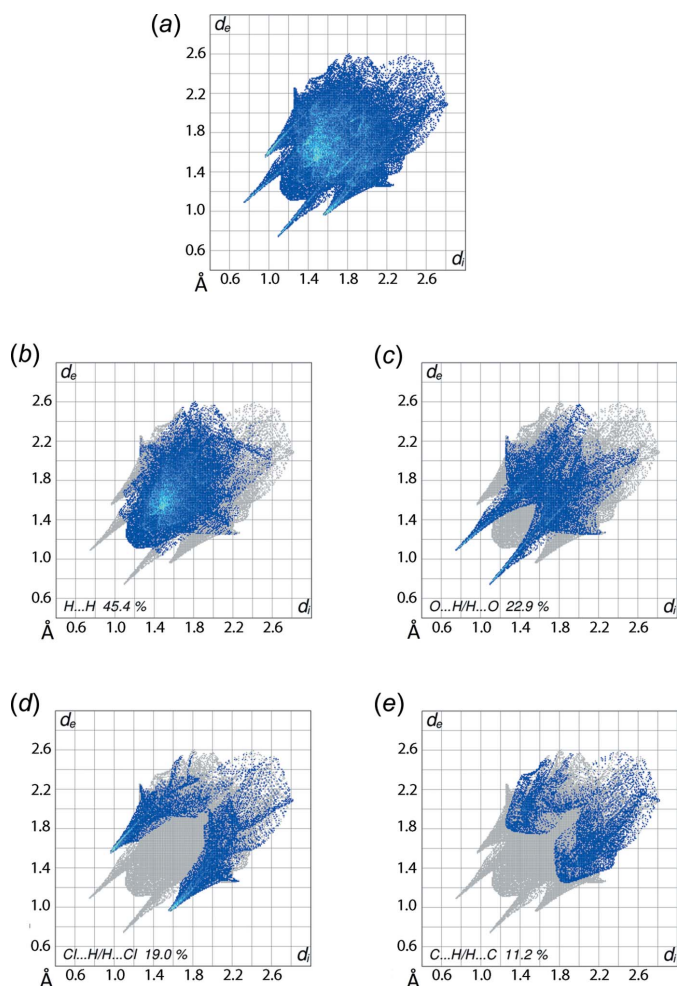
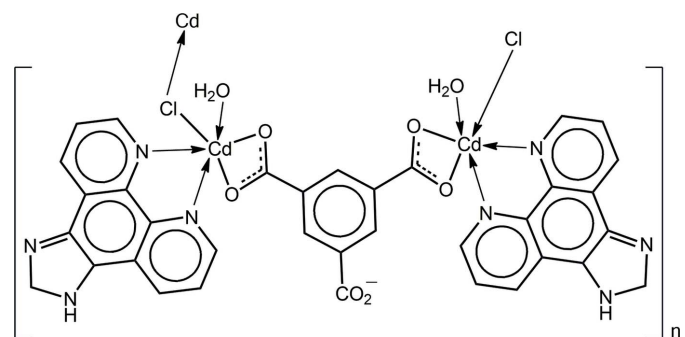


Figure 6
 (a) The full two-dimensional fingerprint plot for (I) and fingerprint plots delineated into (b) H...H, (c) O...H/H...O, (d) Cl...H/H...Cl and (e) C...H/H...C contacts.

involvement of water, diamine, chloride and carboxylate residues in the intermolecular interactions. The relatively high contribution from these atoms decreases the relative importance of interatomic H...H contacts, *i.e.* to 45.4%, to the Hirshfeld surface. The presence of a short interatomic H...H contact between water-H1W and methyl-H3A, Table 4, also has an influence upon the molecular packing as shown in Fig. 5. In the fingerprint plot delineated into H...H contacts, Fig. 6b, this is viewed as the distribution of points at $d_e + d_i < \text{sum of their van der Waals radii}$, *i.e.* 2.40 Å. Another short interatomic H...H contact listed in Table 4, involving benzene-H8 atoms lying at the surfaces of the layers stacked along the *a* axis appear to have little impact upon the packing. The intermolecular O—H...O and N—H...Cl hydrogen bonding are recognized as the pair of spikes at $d_e + d_i \sim 1.8$ and 2.5 Å, respectively, together with green points within the distributions in Fig. 6c and d, respectively. The points related to short inter-atomic O...H contact between water-O1W and methyl-H3A mentioned above are merged in the plot, Fig. 6c. It can be seen from the fingerprint plot delineated into C...H/H...C contacts, Fig. 6e, that although these contacts make a significant contribution of 11.2% to the dumbbell-shaped Hirshfeld surface due to the presence of benzene-C atoms, the molecular packing results in inter-atomic C...H/H...C separations longer than van der Waals contact distances, hence they exert a negligible effect in the crystal. The low contribution from other contacts listed in Table 3 have little effect in the structure due to their large inter-atomic separations.

5. Database survey

A search of the crystallographic literature (Groom *et al.*, 2016) was undertaken in order to find closely related structures to (I). Reflecting the interest in these structures, there were nearly 50 examples with the adipato dianion. In each case, the dianion bridged two Cd^{II} cations *via* chelating interactions in all but one example. Often, the dicarboxylate ligand also bridged other Cd^{II} cations, *i.e.* was found to be coordinating in μ_3 - and μ_4 -modes. The most closely related structure in the literature is illustrated in Scheme 2, *i.e.* (II) (Che *et al.*, 2013).



The coordination geometry for one of the independent Cd^{II} atoms in (II), being defined by two carboxylate-O atoms, derived from a tri-anionic μ_2 -benzene-1,3,5-tricarboxylate ligand, two nitrogen atoms from a chelating imidazo[4,5-*f*]-

Table 5
Experimental details.

Crystal data	
Chemical formula	[Cd ₂ Cl ₂ (C ₆ H ₈ O ₄)(C ₆ H ₈ N ₂) ₂ ·(H ₂ O) ₂]
<i>M_r</i>	692.14
Crystal system, space group	Monoclinic, <i>P2₁/c</i>
Temperature (K)	100
<i>a</i> , <i>b</i> , <i>c</i> (Å)	20.4710 (8), 5.5578 (2), 10.7910 (3)
β (°)	98.122 (3)
<i>V</i> (Å ³)	1215.42 (7)
<i>Z</i>	2
Radiation type	Mo <i>K</i> α
μ (mm ⁻¹)	2.01
Crystal size (mm)	0.33 × 0.22 × 0.10
Data collection	
Diffraction	Agilent Technologies SuperNova Dual diffractometer with Atlas detector
Absorption correction	Multi-scan (<i>CrysAlis PRO</i> ; Agilent, 2013)
<i>T_{min}</i> , <i>T_{max}</i>	0.842, 1.000
No. of measured, independent and observed [<i>I</i> > 2 σ (<i>I</i>)] reflections	15862, 3393, 2992
<i>R_{int}</i>	0.039
(<i>sin</i> θ / λ) _{max} (Å ⁻¹)	0.710
Refinement	
<i>R</i> [<i>F</i> ² > 2 σ (<i>F</i> ²)], <i>wR</i> (<i>F</i> ²), <i>S</i>	0.028, 0.065, 1.04
No. of reflections	3393
No. of parameters	163
No. of restraints	6
H-atom treatment	H atoms treated by a mixture of independent and constrained refinement
$\Delta\rho_{\max}$, $\Delta\rho_{\min}$ (e Å ⁻³)	1.15, -0.69

Computer programs: *CrysAlis PRO* (Agilent, 2013), *SHELXS97* (Sheldrick, 2008), *SHELXL2014* (Sheldrick, 2015), *ORTEP-3 for Windows* (Farrugia, 2012), *DIAMOND* (Brandenburg, 2006) and *pubCIF* (Westrip, 2010).

[1,10]phenanthroline ligand, chlorido and water-O atoms resembles that found in (I); this is illustrated on the left-hand side of Scheme 2. The difference between (I) and (II) is that in (II), the chlorido ligand is bridging, leading to a one-dimensional coordination polymer.

6. Synthesis and crystallization

Benzene-1,2-diamine (0.4324 g, 4 mmol) was slowly added to an aqueous solution (15 ml) of CdCl₂·2H₂O (0.4026 g, 2 mmol) resulting in a yellow solution. The mixture was stirred for about 1 h when adipic acid (0.2923 g, 2 mmol) in MeOH (10 ml) was added. The mixture then was stirred for a further 3 h. The resultant solution was reduced and left for crystallization. Brown crystals of (I) were obtained after a few weeks and analysed directly.

7. Refinement details

Crystal data, data collection and structure refinement details are summarized in Table 5. The carbon-bound H-atoms were placed in calculated positions (C–H = 0.95–0.99 Å) and were included in the refinement in the riding model approximation, with *U*_{iso}(H) set to 1.2*U*_{eq}(C). The O-bound and N-bound H-atoms were located in difference-Fourier maps but were refined with distance restraints of O–H = 0.84 ± 0.01 Å and N–H = 0.88 ± 0.01 Å, and with *U*_{iso}(H) set to 1.5*U*_{eq}(O) and 1.2*U*_{eq}(N). The maximum and minimum residual electron density peaks of 1.15 and 0.69 e Å⁻³, respectively, were located 0.90 and 0.87 Å from the Cd^{II} cation.

Acknowledgements

We are grateful to the University of Malaya's Postgraduate Research Grant scheme (PPP) for Grant No. PG056–2013B.

References

- Agilent (2013). *CrysAlis PRO*. Agilent Technologies Inc., Santa Clara, CA, USA.
- Brandenburg, K. (2006). *DIAMOND*. Crystal Impact GbR, Bonn, Germany.
- Chai, J., Lai, C. S., Yan, J. & Tiekink, E. R. T. (2003). *Appl. Organomet. Chem.* **17**, 249–250.
- Che, G.-B., Wang, S.-S., Zha, X.-L., Li, X.-Y., Liu, C.-B., Zhang, X.-J., Xu, Z.-L. & Wang, Q. W. (2013). *Inorg. Chim. Acta*, **394**, 481–487.
- Farrugia, L. J. (2012). *J. Appl. Cryst.* **45**, 849–854.
- Groom, C. R., Bruno, I. J., Lightfoot, M. P. & Ward, S. C. (2016). *Acta Cryst. B* **72**, 171–179.
- Jotani, M. M., Poplalkhin, P., Arman, H. D. & Tiekink, E. R. T. (2017). *Z. Kristallogr.* **232**, 287–298.
- Lai, C. S. & Tiekink, E. R. T. (2004). *CrystEngComm*, **6**, 593–605.
- Lai, C. S. & Tiekink, E. R. T. (2006). *Z. Kristallogr.* **221**, 288–293.
- Lestari, W. W., Streit, H. C., Lönnecke, P., Wickleder, C. & Hey-Hawkins, E. (2014). *Dalton Trans.* **43**, 8188–8195.
- McKinnon, J. J., Jayatilaka, D. & Spackman, M. A. (2007). *Chem. Commun.* pp. 3814.
- Seco, J. M., Rodríguez-Diéguez, A., Padro, D., García, J. A., Ugalde, J. M., San Sebastian, E. & Cepeda, J. (2017). *Inorg. Chem.* **56**, 3149–3152.
- Sheldrick, G. M. (2008). *Acta Cryst. A* **64**, 112–122.
- Sheldrick, G. M. (2015). *Acta Cryst. C* **71**, 3–8.
- Tan, Y. S., Azizuddin, A. D., Campian, M. V., Haiduc, I. & Tiekink, E. R. T. (2016). *Z. Kristallogr.* **231**, 155–165.
- Tan, Y. S., Halim, S. N. A. & Tiekink, E. R. T. (2016). *Z. Kristallogr.* **231**, 113–126.
- Tan, Y. S., Sudlow, A. L., Molloy, K. C., Morishima, Y., Fujisawa, K., Jackson, W. J., Henderson, W., Halim, S. N. Bt A., Ng, S. W. & Tiekink, E. R. T. (2013). *Cryst. Growth Des.* **13**, 3046–3056.
- Westrip, S. P. (2010). *J. Appl. Cryst.* **43**, 920–925.
- Xue, L.-P., Li, Z.-H., Ma, L.-F. & Wang, L.-Y. (2015). *CrystEngComm*, **17**, 6441–6449.

supporting information

Acta Cryst. (2017). E73, 1363-1367 [https://doi.org/10.1107/S2056989017011677]

(μ_2 -Adipato- $\kappa^4O,O':O'',O'''$)bis[aqua(benzene-1,2-diamine- κ^2N,N')chloridocadmium]: crystal structure and Hirshfeld surface analysis

Wannur Sofiasalamah Khairiah A. Rahman, J. Ahmad, Siti Nadiah Abdul Halim, Mukesh M. Jotani and Edward R. T. Tiekink

Computing details

Data collection: *CrysAlis PRO* (Agilent, 2013); cell refinement: *CrysAlis PRO* (Agilent, 2013); data reduction: *CrysAlis PRO* (Agilent, 2013); program(s) used to solve structure: *SHELXS97* (Sheldrick, 2008); program(s) used to refine structure: *SHELXL2014* (Sheldrick, 2015); molecular graphics: *ORTEP-3 for Windows* (Farrugia, 2012) and *DIAMOND* (Brandenburg, 2006); software used to prepare material for publication: *publCIF* (Westrip, 2010).

(μ_2 -Adipato- $\kappa^4O,O':O'',O'''$)bis[aqua(benzene-1,2-diamine- κ^2N,N')chloridocadmium]

Crystal data

[Cd₂Cl₂(C₆H₈O₄)(C₆H₈N₂)₂(H₂O)₂]

$M_r = 692.14$

Monoclinic, $P2_1/c$

$a = 20.4710$ (8) Å

$b = 5.5578$ (2) Å

$c = 10.7910$ (3) Å

$\beta = 98.122$ (3)°

$V = 1215.42$ (7) Å³

$Z = 2$

$F(000) = 684$

$D_x = 1.891$ Mg m⁻³

Mo $K\alpha$ radiation, $\lambda = 0.71073$ Å

Cell parameters from 7493 reflections

$\theta = 3.8$ – 30.0 °

$\mu = 2.01$ mm⁻¹

$T = 100$ K

Prism, brown

$0.33 \times 0.22 \times 0.10$ mm

Data collection

Agilent Technologies SuperNova Dual diffractometer with Atlas detector

Radiation source: SuperNova (Mo) X-ray Source

Mirror monochromator

Detector resolution: 10.4041 pixels mm⁻¹

ω scan

Absorption correction: multi-scan (CrysAlis PRO; Agilent, 2013)

$T_{\min} = 0.842$, $T_{\max} = 1.000$

15862 measured reflections

3393 independent reflections

2992 reflections with $I > 2\sigma(I)$

$R_{\text{int}} = 0.039$

$\theta_{\max} = 30.3$ °, $\theta_{\min} = 3.0$ °

$h = -28 \rightarrow 26$

$k = -7 \rightarrow 7$

$l = -14 \rightarrow 14$

Refinement

Refinement on F^2

Least-squares matrix: full

$R[F^2 > 2\sigma(F^2)] = 0.028$

$wR(F^2) = 0.065$

$S = 1.04$

3393 reflections

163 parameters

6 restraints

H atoms treated by a mixture of independent and constrained refinement

$w = 1/[\sigma^2(F_o^2) + (0.0312P)^2 + 0.8274P]$

where $P = (F_o^2 + 2F_c^2)/3$

$(\Delta/\sigma)_{\max} < 0.001$

$\Delta\rho_{\max} = 1.15$ e Å⁻³

$\Delta\rho_{\min} = -0.69$ e Å⁻³

Special details

Geometry. All esds (except the esd in the dihedral angle between two l.s. planes) are estimated using the full covariance matrix. The cell esds are taken into account individually in the estimation of esds in distances, angles and torsion angles; correlations between esds in cell parameters are only used when they are defined by crystal symmetry. An approximate (isotropic) treatment of cell esds is used for estimating esds involving l.s. planes.

Fractional atomic coordinates and isotropic or equivalent isotropic displacement parameters (\AA^2)

	<i>x</i>	<i>y</i>	<i>z</i>	$U_{\text{iso}}^*/U_{\text{eq}}$
Cd	0.20549 (2)	0.38825 (3)	0.25421 (2)	0.01173 (6)
Cl1	0.26037 (3)	0.56615 (11)	0.45833 (5)	0.01653 (13)
O1	0.14096 (9)	0.7293 (3)	0.19608 (15)	0.0172 (4)
O2	0.13895 (9)	0.4366 (3)	0.05909 (15)	0.0155 (4)
O1W	0.12696 (9)	0.1564 (3)	0.31419 (16)	0.0155 (4)
H1W	0.1293 (15)	0.026 (3)	0.277 (3)	0.023*
H2W	0.1321 (15)	0.127 (5)	0.3906 (11)	0.023*
N1	0.28158 (11)	0.0464 (4)	0.26867 (19)	0.0149 (4)
H1N	0.2813 (14)	−0.063 (4)	0.327 (2)	0.018*
H2N	0.2722 (14)	−0.009 (5)	0.1919 (14)	0.018*
N2	0.29273 (11)	0.4407 (4)	0.12990 (19)	0.0145 (4)
H3N	0.2803 (13)	0.324 (4)	0.078 (2)	0.017*
H4N	0.2981 (14)	0.582 (3)	0.097 (3)	0.017*
C1	0.12011 (12)	0.6431 (5)	0.0893 (2)	0.0147 (5)
C2	0.07303 (14)	0.7824 (6)	−0.0037 (2)	0.0240 (6)
H2A	0.0485	0.6667	−0.0627	0.029*
H2B	0.0991	0.8867	−0.0526	0.029*
C3	0.02372 (12)	0.9371 (5)	0.0503 (2)	0.0165 (5)
H3A	0.0476	1.0597	0.1059	0.020*
H3B	−0.0018	0.8357	0.1017	0.020*
C4	0.34453 (12)	0.1628 (4)	0.2844 (2)	0.0133 (5)
C5	0.35047 (13)	0.3687 (4)	0.2120 (2)	0.0146 (5)
C6	0.40716 (12)	0.5067 (5)	0.2319 (2)	0.0169 (5)
H6	0.4112	0.6456	0.1822	0.020*
C7	0.45817 (13)	0.4418 (5)	0.3248 (2)	0.0202 (5)
H7	0.4972	0.5360	0.3387	0.024*
C8	0.45193 (13)	0.2395 (5)	0.3971 (2)	0.0210 (5)
H8	0.4866	0.1973	0.4616	0.025*
C9	0.39589 (13)	0.0984 (5)	0.3766 (2)	0.0177 (5)
H9	0.3925	−0.0421	0.4254	0.021*

Atomic displacement parameters (\AA^2)

	U^{11}	U^{22}	U^{33}	U^{12}	U^{13}	U^{23}
Cd	0.01482 (10)	0.00958 (9)	0.01025 (9)	0.00074 (6)	−0.00008 (6)	0.00069 (6)
Cl1	0.0255 (3)	0.0120 (3)	0.0112 (2)	−0.0020 (2)	−0.0006 (2)	−0.0006 (2)
O1	0.0224 (9)	0.0157 (9)	0.0127 (8)	0.0044 (7)	−0.0005 (7)	−0.0009 (7)
O2	0.0200 (9)	0.0150 (9)	0.0111 (8)	0.0031 (7)	0.0007 (7)	−0.0010 (6)
O1W	0.0210 (9)	0.0138 (9)	0.0114 (8)	−0.0019 (7)	0.0015 (7)	0.0002 (7)

N1	0.0212 (11)	0.0123 (10)	0.0109 (9)	-0.0019 (8)	0.0014 (8)	0.0008 (8)
N2	0.0214 (11)	0.0097 (10)	0.0119 (9)	-0.0005 (8)	0.0007 (8)	0.0027 (8)
C1	0.0156 (12)	0.0162 (12)	0.0123 (11)	0.0028 (9)	0.0027 (9)	0.0018 (9)
C2	0.0267 (14)	0.0310 (16)	0.0133 (11)	0.0147 (12)	0.0000 (10)	0.0009 (11)
C3	0.0189 (13)	0.0156 (12)	0.0140 (11)	0.0057 (10)	-0.0018 (9)	0.0008 (9)
C4	0.0161 (12)	0.0124 (11)	0.0117 (10)	0.0026 (9)	0.0025 (9)	-0.0016 (9)
C5	0.0185 (12)	0.0145 (12)	0.0112 (11)	0.0027 (9)	0.0027 (9)	-0.0012 (9)
C6	0.0206 (13)	0.0132 (12)	0.0174 (12)	0.0010 (10)	0.0047 (9)	-0.0011 (9)
C7	0.0164 (13)	0.0221 (14)	0.0222 (13)	-0.0039 (10)	0.0038 (10)	-0.0035 (11)
C8	0.0173 (12)	0.0259 (15)	0.0188 (12)	0.0061 (11)	-0.0010 (9)	-0.0014 (10)
C9	0.0221 (13)	0.0165 (13)	0.0148 (12)	0.0042 (10)	0.0034 (10)	0.0014 (9)

Geometric parameters (Å, °)

Cd—O1	2.3448 (17)	C2—C3	1.505 (4)
Cd—O2	2.3560 (16)	C2—H2A	0.9900
Cd—N1	2.448 (2)	C2—H2B	0.9900
Cd—N2	2.398 (2)	C3—C3 ⁱ	1.521 (5)
Cd—C11	2.5283 (6)	C3—H3A	0.9900
Cd—O1W	2.2265 (18)	C3—H3B	0.9900
O1—C1	1.265 (3)	C4—C9	1.389 (3)
O2—C1	1.268 (3)	C4—C5	1.400 (3)
O1W—H1W	0.834 (10)	C5—C6	1.382 (4)
O1W—H2W	0.832 (10)	C6—C7	1.389 (4)
N1—C4	1.430 (3)	C6—H6	0.9500
N1—H1N	0.875 (10)	C7—C8	1.385 (4)
N1—H2N	0.879 (10)	C7—H7	0.9500
N2—C5	1.431 (3)	C8—C9	1.381 (4)
N2—H3N	0.871 (10)	C8—H8	0.9500
N2—H4N	0.874 (10)	C9—H9	0.9500
C1—C2	1.504 (3)		
O1W—Cd—O1	98.22 (6)	O2—C1—C2	118.9 (2)
O1W—Cd—O2	88.62 (6)	O1—C1—Cd	59.78 (12)
O1—Cd—O2	55.66 (6)	O2—C1—Cd	60.29 (12)
O1W—Cd—N2	149.12 (7)	C2—C1—Cd	179.18 (18)
O1—Cd—N2	100.84 (7)	C1—C2—C3	116.0 (2)
O2—Cd—N2	82.44 (7)	C1—C2—H2A	108.3
O1W—Cd—N1	90.66 (7)	C3—C2—H2A	108.3
O1—Cd—N1	166.89 (6)	C1—C2—H2B	108.3
O2—Cd—N1	115.34 (6)	C3—C2—H2B	108.3
N2—Cd—N1	67.19 (7)	H2A—C2—H2B	107.4
O1W—Cd—C11	102.90 (5)	C2—C3—C3 ⁱ	112.5 (3)
O1—Cd—C11	94.65 (4)	C2—C3—H3A	109.1
O2—Cd—C11	149.72 (5)	C3 ⁱ —C3—H3A	109.1
N2—Cd—C11	99.52 (5)	C2—C3—H3B	109.1
N1—Cd—C11	92.72 (5)	C3 ⁱ —C3—H3B	109.1
C1—O1—Cd	92.43 (14)	H3A—C3—H3B	107.8

C1—O2—Cd	91.84 (14)	C9—C4—C5	119.6 (2)
Cd—O1W—H1W	106 (2)	C9—C4—N1	123.1 (2)
Cd—O1W—H2W	114 (2)	C5—C4—N1	116.8 (2)
H1W—O1W—H2W	107 (3)	C6—C5—C4	120.3 (2)
C4—N1—Cd	102.19 (15)	C6—C5—N2	122.9 (2)
C4—N1—H1N	109.0 (19)	C4—C5—N2	116.4 (2)
Cd—N1—H1N	121 (2)	C5—C6—C7	119.8 (2)
C4—N1—H2N	110.0 (19)	C5—C6—H6	120.1
Cd—N1—H2N	99 (2)	C7—C6—H6	120.1
H1N—N1—H2N	115 (3)	C8—C7—C6	119.8 (2)
C5—N2—Cd	103.59 (14)	C8—C7—H7	120.1
C5—N2—H3N	109 (2)	C6—C7—H7	120.1
Cd—N2—H3N	95.4 (19)	C9—C8—C7	120.8 (2)
C5—N2—H4N	111.2 (19)	C9—C8—H8	119.6
Cd—N2—H4N	119 (2)	C7—C8—H8	119.6
H3N—N2—H4N	117 (3)	C8—C9—C4	119.7 (2)
O1—C1—O2	120.1 (2)	C8—C9—H9	120.1
O1—C1—C2	121.0 (2)	C4—C9—H9	120.1
Cd—O1—C1—O2	0.2 (2)	C9—C4—C5—N2	-172.4 (2)
Cd—O1—C1—C2	-179.7 (2)	N1—C4—C5—N2	0.0 (3)
Cd—O2—C1—O1	-0.2 (2)	Cd—N2—C5—C6	-130.3 (2)
Cd—O2—C1—C2	179.7 (2)	Cd—N2—C5—C4	42.1 (2)
O1—C1—C2—C3	-34.4 (4)	C4—C5—C6—C7	-0.5 (4)
O2—C1—C2—C3	145.7 (3)	N2—C5—C6—C7	171.6 (2)
C1—C2—C3—C3 ⁱ	-177.6 (3)	C5—C6—C7—C8	-0.1 (4)
Cd—N1—C4—C9	131.4 (2)	C6—C7—C8—C9	1.1 (4)
Cd—N1—C4—C5	-40.8 (2)	C7—C8—C9—C4	-1.5 (4)
C9—C4—C5—C6	0.2 (4)	C5—C4—C9—C8	0.8 (4)
N1—C4—C5—C6	172.6 (2)	N1—C4—C9—C8	-171.1 (2)

Symmetry code: (i) $-x, -y+2, -z$.

Hydrogen-bond geometry (\AA , $^\circ$)

$D-H\cdots A$	$D-H$	$H\cdots A$	$D\cdots A$	$D-H\cdots A$
O1W—H1W \cdots O1 ⁱⁱ	0.83 (2)	1.90 (2)	2.728 (2)	176 (3)
O1W—H2W \cdots O2 ⁱⁱⁱ	0.83 (1)	1.84 (1)	2.670 (2)	177 (3)
N1—H1N \cdots Cl1 ⁱⁱ	0.88 (2)	2.57 (2)	3.428 (2)	166 (2)
N1—H2N \cdots Cl1 ^{iv}	0.88 (2)	2.52 (2)	3.374 (2)	165 (2)
N2—H3N \cdots Cl1 ^{iv}	0.87 (2)	2.53 (2)	3.385 (2)	168 (2)
N2—H4N \cdots Cl1 ^v	0.88 (2)	2.52 (2)	3.322 (2)	153 (3)

Symmetry codes: (ii) $x, y-1, z$; (iii) $x, -y-1/2, z-1/2$; (iv) $x, -y-1/2, z-3/2$; (v) $x, -y+1/2, z-3/2$.